Journal of Science and Sustainable Development (JSSD), 2025, 13(2), 54-71

ISSN: 2304-2702 (print); 2414-4479 (online)
DOI: https://doi.org/10.20372/au.jssd.13.2.2025.0649

RESEARCH PAPER

Preparation and Characterization of Activated Carbon from Root and Inflorescence of Enset/*Ensete-Vetricosum*/ for the Removal Pb(II) from Aqueous Solution

Abdisa Gebisa Jebessa*, Ejere Leta Megenasa and Bekele Negassa Sesaba
Department of Chemistry, Natural and Computational Science College, Ambo University

***Corresponding Author:** Email: abdisachemist@gmail.com*

Abstract

Activated carbon was synthesized from the inflorescence and root of enset/ensete vetricosum to effectively remove Pb(II) heavy metal ions from aqueous solutions. The process involved chemical activation using H_3PO_4 followed by carbonization at 300°C for 15 minutes. The most effective conditions for creating activated carbon varied depending on the source material. For enset inflorescence (flower), a preparation temperature of 25°C, a pH of 5, and a contact time of 60 minutes yielded the good results. In contrast, the optimal conditions for preparing activated carbon from enset root were a temperature of 30°C, a neutral pH of 7, and a shorter contact time of 30 minutes. Adsorbent doses of 1.5 g and 2 g in 200 mL solution were found to be optimal. The adsorption capacities for Pb(II) by inflorescence and root were determined to be 1.36 mg/g and 1.68 mg/g, respectively. Freundlich adsorption isotherm models provided better fits for the experimental adsorption equilibrium data compared to Langmuir models. FT-IR spectra analysis revealed the presence of functional groups responsible for binding Pb(II) ions onto the adsorbent. Kinetics data suggested that the pseudo-second order model best described the adsorption process. The synthesized activated carbon showed high efficiency in removing Pb(II) ions from aqueous solutions, making it a promising adsorbent for Pb(II) and related heavy metal removal.

Keywords: Adsorption, heavy metals, Langmuir-Freundlich isotherm models, adsorption kinetics

Introduction

Ensete ventricosum, is a notable monocarpic perennial that considered to the family Musaceae which also includes bananas (*Musa spp.*). Originating in Ethiopia, this species has been uniquely domesticated, and as a result, it holds immense cultural, agricultural, and economic significance. Furthermore, it serves as a primary staple food for approximately 20 million people, particularly in the densely populated south and southwestern highlands (Kidane *et al*., 2021).

Researches indicates that different Enset landraces show variations in the nutritional content of their corms, which include considerable amounts of carbohydrates, fiber, and essential minerals such as iron and zinc (Kidane *et al*., 2021). The inflorescence of enset, characterized by a large drooping flower spike, plays a vital role in food production. Specifically, the stalk of the inflorescence, along with the pseudos' term and corm, undergoes processing to produce "kocho" and "bulla." Kocho is made from the fermented pulp, while bulla is a refined starch extracted from the liquid of the pulverized mixture.

Together, these products highlight the importance of enset in the local diet and economy (Kidane *et al*., 2021).

Traditionally, Enset plants are often harvested prior to flowering to optimize the starch content in the vegetative parts (Kidane *et al*., 2021). Unlike its banana relatives, Enset is not cultivated for its fruit, which is small, inedible, and contains hard seeds. Instead, various parts of the plant, including the root (corm) and the inflorescence stalk, are crucial sources of sustenance and have diverse traditional uses (mohammed and Chala, 2014). Studies have demonstrated the effectiveness of activated carbon produced from Activated carbon made from *Ensete ventricosum* leaves effectively removes organic pollutants like phenol from water. When prepared under optimized conditions (considering factors like carbonization temperature, activation agent, and impregnation ratio), this activated carbon exhibits a high surface area and excellent adsorption capabilities (Keder, 2023). This offers a sustainable and environmentally friendly way to treat industrial wastewater.

One of the biggest threats to human health is contaminated water, which is also inappropriate for residential usage. Natural or man-made processes, such as the release of heavy metals into soils and water supplies through the disposal of wastewater, can be the source of contaminated water. Because heavy metals are hazardous to a wide variety of living species, their presence in the environment is a serious concern (Alloway, 2013). These compounds may be the result of pesticide and fertilizer use in agriculture, urban or industrial pollution, or both (WHO, 2011). The effects of toxic contamination on the environment might be either acute or chronic (long-term). This frequently goes above the allowable sanitary norms, which has a negative effect on groundwater and the aquatic environment, as well as on human health (Vasseur, 2008). According to Dagmawi *et al*. (2013), 70% of industrial effluents in developing nations are discharged into the surrounding environment untreated.

Many water bodies are receiving doses of heavy metals from increased industrial activity that surpass the maximum allowable limit for wastewater discharge intended to safeguard people, animals, and the environment (Iqual and Saeed, 2007). Toxic heavy metals are not biodegradable, which is a major concern were also discharge in the environment in many cases. Moreover, they react irreversibly with enzymes and proteins, further complicating their impact on biological systems. Their strength as strong oxidants allows them to be absorbed through the skin, leading to a variety of disorders and diseases (Jaishankar *et al*., 2014; Nordberg *et al*., 2007).

There are several methods for removing these toxic heavy metals, which can be broadly categorized into three groups: chemical, biological, and physical. Each method offers distinct benefits and drawbacks depending on its application. Notably, the World Health Organization (WHO) identifies chromium (Cr), copper (Cu), zinc (Zn), iron (Fe), cadmium (Cd), mercury (Hg), and lead (Pb) as the metals of greatest concern for public health at present (Muhammad *et al.,* 2004).

These metals are not easily detoxified or broken down by the body, and has degree of accumulate in living organisms. Therefore, when selecting appropriate treatment procedures, it is crucial to consider the need to enhance effluent discharge standards to protect the environment. Nowadays, there is a growing emphasis on using environmentally friendly treatment techniques. Furthermore, utilizing certain waste materials that may be beneficial in this context, along with their reuse, can provide a significant advantage (Jaishankar *et al*., 2014).

Research on the application of suitable and affordable technologies for the purification of drinking water in poor nations has been conducted recently. Additionally, studies have concentrated on domestic production of water treatment chemicals using locally sourced raw ingredients (Warhurst *et al.,* 1997).

Adsorption is one of these methods. By using byproducts as starting points to make

commonly used adsorbents, like activated carbons, it is possible to add value to the total amount of biomass gathered. The amount of safe drinking water that is available to the public is limited in most poor nations due to the high expense of importing activated carbon. Wood, lignite, peat, and coal are examples of raw materials having a high carbon content but a low inorganic content that can be used to produce adsorbents like activated carbon (AC) for adsorption (Jabit, 2007).

Carbon precursors can be derived from a broad variety of carbonaceous sources, including wood, coal, peat, and different agricultural byproducts. Due to their widespread availability, affordability, and renewability, agricultural byproducts have drawn more attention lately for the production of activated carbon (Kadirvelu *et al*., 2003). It is evident from many literary works that a wide species of materials are utilized to manufacture activated carbon for adsorption applications. These include wood sawdust (Bogdanka, 2007), teff straw (Mulu, 2013), rice husk (Srivastava et al., 2015), sugarcane bagasse (Kalderis *et al*., 2008), coffee husk (Kanamadi et al., 2010), and other industrial waste (Kadirvelu *et al.,* 2001). As the reports confirmed on the use of enset root and inflorescence's activated carbon as sorption qualities for Pb(II) removals in aqueous solutions. Thus, this study aims to construct and assess enset root and inflorescence adsorption effectiveness for absorbent of Pb(II) from aqueous solutions.

Materials and Methods

Instruments and Equipment

The Fourier Transform Infrared (FT-IR) spectrophotometer (Model: IR Affinity 1S class 1), UV/Vis-SP65 SYANO spectrophotometer, atomic absorption spectroscopy (AAS), Agilent -2000) are used.

Chemicals and Reagents

Analytical-grade chemicals, such as PbNO3 for standard metal ion sample preparation, H3PO4 as an enset root activation agent, and the inflorescence-activated carbon generation procedure, were employed in this investigation. Distilled water was utilized in all trials to get rid of any remaining acid char. For adjusting pH, use NaOH and HCl. All of the solutions used in the experiment were made with distilled water.

Experimental Methods and Procedures

Raw Material Preparation

Enset root and flower were Randomly obtained from a nearby community house in Ambo town, West Shoa, Ethiopia, in order to prepare adsorbents. This settlement is situated in the West Showa of the Oromia Region, west of Addis Ababa. Its elevation is 2101 meters, and its latitude and longitude are 8°59′ N and 37°51′ E. After being cut off from other components, the root and inflorescence were thoroughly cleaned with tap water multiple times to get rid of dirt, dust, and other contaminants. It was repeatedly cleaned with distilled water. After the separated root and inflorescence were chopped into tiny pieces, they were dried for a week in the sun and then for 24 hours at 105 °C in an oven to get rid of any moisture.

The inflorescence and enset root were chosen f or the activated carbon preparation process. For future research, the dried materials were kept in a sterile area in sealed plastic bags.

Figure 1. Pretreatment of enset root and inflorescence

Preparation of Activated Carbon

Before carbonization, the dried samples were oven-dried for 12 hours at 105 °C to eliminate any remaining moisture (Figure 1). Phosphoric acid was added to the samples after they were taken out of the crucible and cooked in the electrical furnace. For fifteen minutes, the oven was kept at 300 °C, during which time carbon was produced. Once the activated carbon had cooled to room temperature, it was carefully cleaned with distilled water until the pH of the effluent, or supernatant, stabilized at a value close to neutral. The samples were then dried for 12 hours at 105 °C (Figure 2). Lastly, the inexpensive activated carbon made from the root and inflorescence was crushed and kept in a ready-made sample holder until needed for next steps.

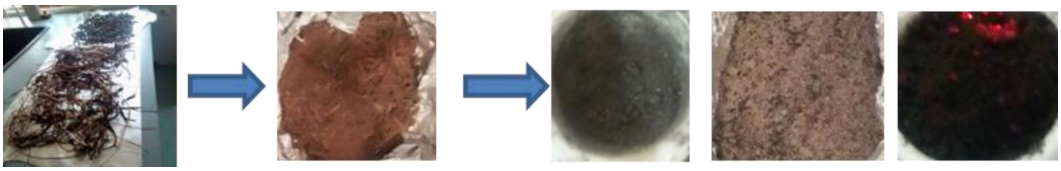

Figure 2. Enset root and Inflorescence stem activation

Characterization of Prepared Activated Carbon

FT-IR Spectroscopy

Enset root and inflorescence, low-cost ACs, and metal-loaded Enset root and inflorescence prepared ACs treatment experimental were performed differently and FTIR absorption for different functional groups scanned in the spectral range of 400 – 4000 cm^{-1} region.

FTIR of Enset Root and Inflorescence Activated Carbon

For the enset root and inflorescence activated carbon transform FT-IR, spectrum analyses were performed. The sample disks were filled with a tablet form of the sorbent for this investigation, and the activated carbon spectra were recorded. Using a screw and a pair of metal dies, the sample was squeezed into a pellet on a 7-mm collar. With the use of a screw, the collar holding the pellet was taken out of the metal die and put inside a cuvette. After turning on the device, the samples were scanned. Distinct linkages in various functional groups were found to correspond to distinct bands in the spectrum

FTIR of Metal Loaded Enset Root and Inflorescence Activated Carbon

After adsorption and filtering, the enset root and inflorescence waste were dried at 105 ^0C in an oven for 24h to eliminate any moisture. 0.5 grams of dry metal-loaded fractions using a mortar and pestle, the enset root and inflorescence were mashed into a powder. Using a mortar and pestle, the fine powder was combined with 1.0 g of analytical-grade KBr. The blend was ground finely. The sample was positioned on a 7-mm collar and compressed using a screw and a series of metal dies to create a pellet. After being taken out of the metal dye and set on the sample container, the collar holding the pellet was replaced. After turning on the equipment, the sample was analyzed. The spectra of enset root and inflorescence of ACs were recorded in specified region.

Preparation of Adsorbate Solution

To ensure accurate results, 1.6 g of $Pb(NO_3)_2$ was dissolved in 1L of distilled water using a volumetric flask to prepare a stock Pb(II) solution with a concentration of 1 g/L. This stock solution was then diluted using double deionized water to obtain the required concentrations. Serial dilutions of the stock solution were performed to produce the working solutions. These working solutions were prepared in 250 mL Erlenmeyer flasks by adjusting the stock solution with deionized water to achieve the desired concentrations.

The adsorbate solutions were prepared at four specific concentrations: 20, 30, 40, and 50 ppm. The dilution equation was applied to calculate the concentrations of these working solutions based on the original stock solution.

Calibration of Pb(II) Absorbance

The amounts of metals in the activated carbon were measured using an Agilent Technologies 200 series atomic absorption spectrophotometer. Prior to the sample determination, the instruments were calibrated using the standards. Both the regular functioning solution and the approaches have blank solutions ready. 10 mL of the standard $Pb(NO_3)_2$ were calibrated appropriately as per needed in order to prepare 100 ppm. Distilled with deionized water at the end, and the mixture was well combined. By pipetting the 100 ppm standard working solution into calibrated flasks and adding deionized water to fill the capacity, the solution was made ready.

Batch Adsorption Experiment

The batch experiment was conducted at ambient temperature by introducing a measured amount of sample powder into 250 mL conical flasks containing Pb(II) solutions. Each mixture was then shaken at a constant speed of 200 rpm for designated time intervals. Following agitation, the solid material was separated through filtration using Whatman No. 1 filter paper. The experiment involved varying the initial metal ion concentrations, pH levels, and the quantity of Enset root and inflorescence applied for adsorption. After the adsorption process, each suspension was filtered, and the resulting filtrates were analyzed to determine the concentration of the respective metal ions.

The removal efficiency of Pb(II) ions from aqueous solution calculated as equation 3.1

$$\%\text{Removal} = (Co - Cf)/Co \times 100 \quad \text{.....3.1}$$

Where Co and Cf ; initial and final concentration (mgL^{-1}) of metal ion respectively

Batch adsorption experiment of Pb(II) performed to determine the adsorption degree of enset root and inflorescence at different metals concentrations.

The initial and final concentrations of the solutions were measured and quantified using AAS at λ_{max}, and the adsorption capacities of the adsorbents were calculated accordingly. The adsorption capacities of the adsorbents used in this study were quantified using the following equation:

$$q = \left(\frac{Co - Ct}{W}\right) V \qquad 3.2$$

Where V is volume (L), C_0 and C_e are initial and equilibrium concentrations (mg/L), and W is adsorbent weight (g).

The influence of solution pH, Pb(II) concentration, adsorbent dosage, and contact time on the adsorption efficiency of the synthesized ACs was systematically examined using central composite design to identify the optimal adsorption conditions.

Factors Affecting the Batch Equilibrium Studies

Effect of Contact Time

To determine the adsorption rate of Pb(II) ions using low-cost activated carbon derived from enset root and inflorescence, 50 mL of standard solutions were used, and the amount of metal ions adsorbed was measured at different contact times: 30, 60, 90, and 120 minutes. During the experiment, temperature, initial concentration, and pH were maintained constant (Shan *et al.,* 2007).

Effect of Activated Carbon Dosage

The effect of adsorbent dosage on metal ion removal was investigated by adding 0.5, 1.0, 1.5, and 2.0 grams of activated carbon into separate 250 mL Erlenmeyer flasks, each containing a metal ion solution with a concentration of 40 mg/L. The adsorption efficiency for each dosage was then evaluated under constant temperature, contact time, and pH conditions.

Effect of pH

To assess how solution acidity affects adsorption efficiency, the pH of Pb(II) solutions was adjusted between 1 and 10 at two-unit intervals. During these experiments, temperature and metal ion concentration were kept constant. Pavasant *et al*., 2006). Adsorption experiments were carried out by temperature and concentration remains constant.

Effect of Initial Concentration of Adsorb Ate

This stage evaluates how different metal ion concentrations impact the removal efficiency of the adsorbent (low-cost activated carbon from enset root and inflorescence). The effect was tested using metal ion concentrations of 20, 30, 40, and 50 mg/L, while all other conditions were maintained constant.

Effects of temperature

The impact of temperature on Pb(II) removal was examined by conducting experiments at different temperatures (25, 30, 35, and 40°C) for a duration of one hour. A temperature-controlled shaker was used to maintain the desired temperatures.

The Study of Heavy Metal Adsorption kinetics

Studying adsorption kinetics is essential as it offers insight into the adsorption mechanism and behavior, which are critical for evaluating process efficiency. In this research, pseudo-first-order and second order kinetics model were studied. These models were applied at various concentrations to identify which one best aligns with the experimental adsorption capacity values. This analysis helps determine the sorption model that the system follows. Mathematically pseudo-first order is expressed as

$$\text{Log}\,(q_e\text{-}q_t) = \log q_e - \frac{k1t}{2.303} \qquad 3.3$$

Here, q_e represents the equilibrium adsorption capacity (mg/g), q_t is the adsorption capacity at time t, and k is the pseudo-first-order rate constant (g/mg·h), which can be determined from a plot of $\log(q_e - q_t)$. The pseudo-second-order kinetic model is expressed mathematically as follows:

$$1/qt = 1/k_2qe_2 + t/qe \qquad 3.4$$

Results and Discussions

Characterizations of the Prepared Enset Inflorescence and Root

FT-IR Analysis of Adsorbent

FT-IR spectroscopy was performed to identify the various functional groups present in the adsorbent, as these groups play a key role in the adsorption process. To determine which functional groups in the enset inflorescence are involved in metal ion binding, FT-IR spectra were recorded before (Figure 3a) and after Pb(II) adsorption (Figure 3b) within the range of 4000–400 cm^{-1}. The broad absorption peaks observed at 3331.91 cm^{-1} and 3274 cm^{-1} were attributed to O–H stretching, indicating the presence of intra- and intermolecular hydrogen bonding. The O-H stretching vibrations indicate the presence of free hydroxyl groups and bonded O–H bands of polymeric compounds such as alcohols or phenols, as in pectin, hemicelluloses, cellulose and lignin (Iqbal *et al*., 2008). The peak observed at 2918.17cm^{-1} and 2923.46cm^{-1} was associated with asymmetric C–H stretching vibrations of aliphatic acids (Feng *et al*., 2008).

The peaks observed at 2290 and 2321 cm^{-1} correspond to aliphatic C–H stretching vibrations. The peak at 1153 cm^{-1} is attributed to C–N stretching of amine groups, while the peak at 1041 cm^{-1} is associated with C–O stretching in primary hydroxyl groups. The peak at 1269 cm^{-1} is related to C–O stretching vibrations from alcohols (C–OH). These functional groups are likely involved in the binding of Pb(II) ions.

The corresponding functional groups and the related absorbance peaks data presents in table 1, confirmed the shifting of absorption bands

and the disappearances of absorption bands due to binding with Pb(II) ions in aqueous solutions with the prepared absorbent.

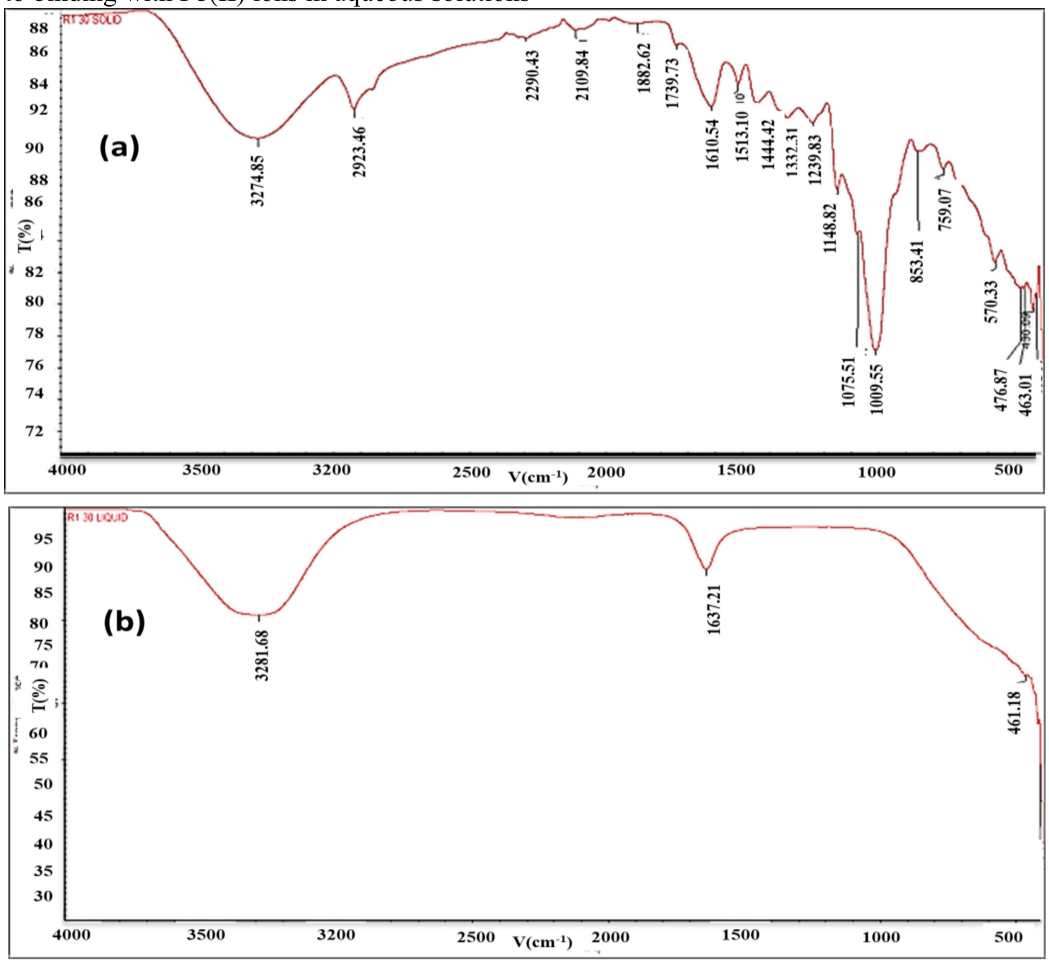

Figure 3. FT-IR spectra of Activate carbon prepared from enset inflorescence (a) before adsorption and (b)after adsorption

Table 1. FTIR spectrum of Enset inflorescence AC before and after adsorption

Frequency(cm^{-1}) before adsorption	Frequency(cm^{-1}) After adsorption	Bond	Functional groups
3274,88	3281	O-H stretching	Hydroxyl
2923.46	--	C-H stretching	Alkanes
1610	1637	C=C stretching	Alkene
1075	---	C-O	Alcohol
1009	--	C-O	Ether

Similar to enset inflorescence the FTIR spectra were recorded in order to quantify which functional groups of enset root responsible for metal uptake, for adsorbent before (Figure 4a) and after Pb(II) binding absorption were scanned (Figure 4b). The broad peak at 3331.91 cm^{-1} and 2918.17 cm^{-1} indicate O-H group presence. The disappearance several absorption peaks from Figure 4b comparing with Figure 4a, confirm the formation of certain binding with Pb(II) and the morphological change of functional group of enset root after treatment

with metal. Similarly, the data presents in table 2, the shifting of absorption bands and the disappearances confirmed the change of functional groups after binding with Pb(II) ions in aqueous solutions.

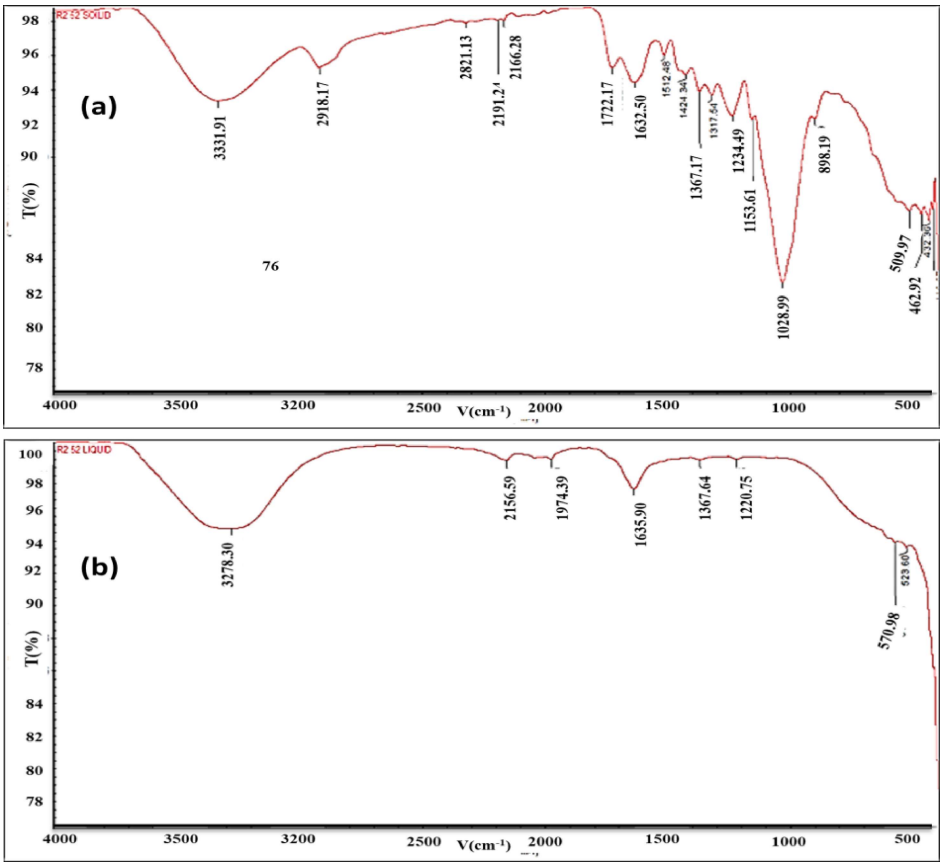

Figure 4. Adsorption spectra of Enset root AC (a) before adsorption and (b) after adsorption

Table 2. FTIR spectrum of root AC before and after adsorption

Frequency(cm^{-1}before adsorption	Frequency(cm^{-1})after adsorption	Bond	Functional groups
3331.5	3278	O-H stretching	Hydroxyl
2918,5	2914	C-H stretching	Alkanes
1635	1632	C=C	Aromatic
1029.99	----	S=O	Sulfoxode

Calibration of Pb(II) Absorbance

An AAS was employed to measure the metal concentrations in the activated carbon samples. Prior to analysis, the instrument was calibrated using standard solutions (Figure 5). A 100 ppm stock solution of each metal was used to prepare a 10 ppm intermediate solution, which was then diluted to create working standards based on the sensitivity of each specific lamp in

the AAS. Calibration was performed using these working standards, resulting in a strong correlation coefficient. Once proper calibration was confirmed, the metal concentrations in the samples were measured. The calibration curves for each metal, showing absorbance versus concentration (mg/L), are presented in Figure 5.

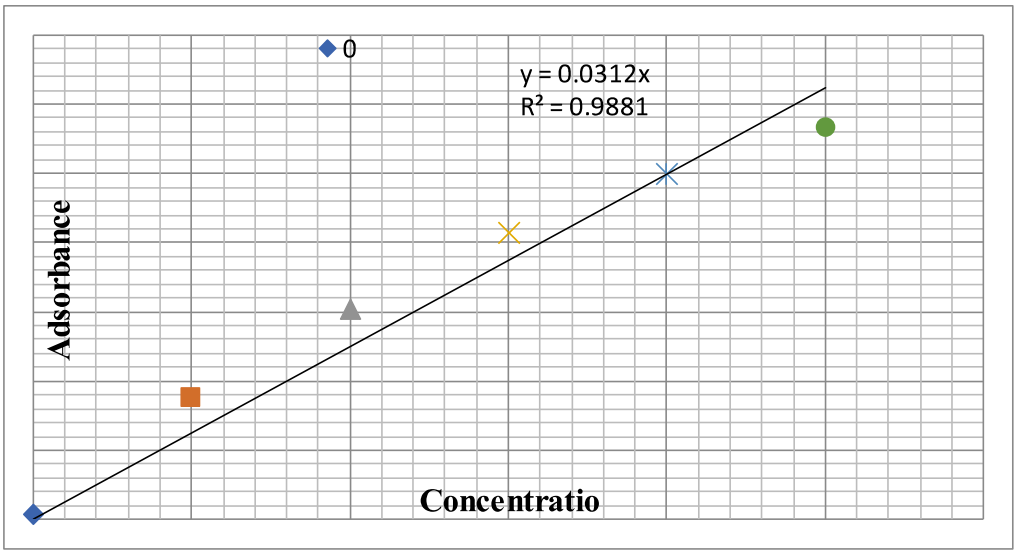

Figure 2. Calibration Curve for Pb(II) ion versus Absorbance

Factors Affecting the Adsorption of Pb(II)

Effect of contact time

In the figure 6a, the influence of contact time for absorption of Pb(II) via keeping other parameters constant at pH 7, Con = 40 mg/L, dose = 0.5 g, agitation speed = 120 rpm) was presented. In order to find out the time required for equilibrium adsorption, the contact time for Pb(II) ions on the enset inflorescence and root were varied as (30, 60, 90, and 120 min) at a fixed Pb(II) ions concentration of 40 ppm, a dosage of adsorbent of 0.5 g per 40 mL solution, at room temperature.

The adsorption reaches a maximum, (99.9 %) at 60 min, but decreases with further elapse of time due to desorption. For enset root the maximum removal efficiency of the metal ions (84.7%) occur at 30 min and decrease with increasing time and percentage removal of enset inflorescence is higher than enset root (99.9% > 84.7%). Hence, the optimum contact time (60 and 30 min) was selected for further experiments.

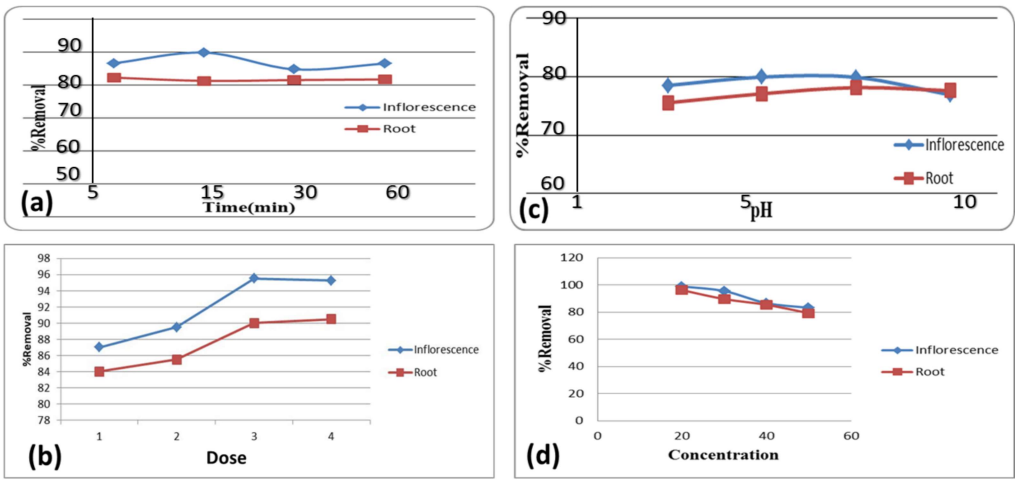

Figure 6. (a) Influence of contact time on the removal efficiency of Pb(II) at different time intervals; (b) Influence of adsorbent dosage on the removal efficiency of Pb(II); (c) Influence of pH on the removal efficiency of Pb(II) at varying pH levels; (d) Influence of initial metal ion concentration on the removal efficiency of Pb(II) from aqueous solution.

Effect of Activated Carbon Dosage

Figure 6b demonstrates how varying the adsorbent dosage influences the adsorption of Pb(II) ions when using activated carbon produced from enset inflorescence and root.

For the activated carbon derived from enset inflorescence, the adsorption of Pb(II) ions initially increased from approximately 87.0% at Dose 1 to 89.5% at dose 2, before subsequently increasing to a maximum of approximately 95.5% at dose 3. This maximum adsorption was observed under the conditions of a fixed Pb(II) ions concentration of 40 ppm, a contact time of 60 min, and a temperature of 25 °C. The most significant increase in percent adsorption (from 89.5% to 95.5%) occurred when the adsorbent dose from dose was increased from dose 2 to dose 3. However, , above this optimal dose 3, the percent adsorption of Pb(II) ions slightly decreased to approximately 95.0% at dose 4.

This non-linear trend observed for the enset inflorescence activated carbon, with an initial increase followed by a subsequent slight decrease in adsorption efficiency with increasing adsorbent dose, warrants further investigation. Potential explanations for this behavior may be agglomeration of adsorbent particles; this means at higher doses beyond the optimum, the activated carbon particles might agglomerate, leading to a reduction in the effective surface area available for adsorption. Additionally, at certain dosages, the activated carbon might release some impurities that compete with Pb(II) ions for adsorption sites, or that the surface chemistry evolves with increasing mass in a complex way.

In contrast, the adsorption of lead ions onto activated carbon derived from enset root exhibited a more typical trend, increasing with the adsorbent dose from approximately 84.0% at Dose 1 to 90.5% at dose 4. This increase was continuous throughout the studied range of doses (1 to 4) under the same fixed conditions of Pb(II) ions concentration (40 ppm), contact time (60 min), and temperature (25 °C). The maximum adsorption within the observed range was achieved at the highest tested adsorbent dose of dose 4, suggesting that within the studied range, more adsorbent consistently provided more available binding sites.

The study indicates that increasing the dose of the enset root-derived adsorbent up to Dose 4 was effective in absorbing a higher number of ions within the experimental parameters. This observation aligns with the general principle that an increased adsorbent dose provides a greater number of active sites, leading to higher

removal efficiency. The peak removal for inflorescence was approximately 95.5%, while for root it reached approximately 90.5%.

Effect of pH

pH plays a crucial role in the adsorption of Pb(II) ions. To realize this, the removal efficiency was examined at different pH values (3, 5, 7, and 9) while keeping the initial Pb(II)ions concentration (40 ppm), adsorption time (60 min), agitation speed (120 rpm), and adsorbent weight (0.5 g) constant for both enset inflorescence and root activated carbons.

Figure 6c illustrates that the adsorption efficiency of Pb(II) ions onto both adsorbents generally increased as the solution pH rose. However, the maximum adsorption wasn't at the highest pH tested. For the enset inflorescence activated carbon, the peak removal efficiency of 99.7% was observed at pH 5, while for the enset root activated carbon, the maximum of 90.7% occurred at pH 7. Beyond these optimal pH values, the adsorption efficiency decreased for both materials.

This suggests that slightly acidic to neutral conditions were most favorable for Pb(II)ions adsorption onto these activated carbons under the tested conditions. Specifically, Figure 6c indicates that the enset inflorescence activated carbon exhibited a better Pb(II)ions removal efficiency than the enset root activated carbon within this slightly acidic to neutral pH range.

Figure 6d shows the impact of varying initial Pb(II) concentrations on the removal efficiency of both enset inflorescence and root activated carbons. These experiments were conducted under consistent conditions: an adsorbent dose of 0.5 g, a pH of 7, a contact time of 60 min, and an agitation speed of 120 rpm for each adsorbent material. The removal efficiency of Pb(II) by the enset inflorescence activated carbon decreased as the initial Pb(II) concentration increased. Specifically, the removal efficiencies were 98.9% at 20 mg/L, 95.5% at 30 mg/L, 86.6% at 40 mg/L, and 83.2% at 50 mg/L. This shows a clear inverse relationship: higher initial Pb(II) concentrations led to a lower percentage of Pb(II) removed by the inflorescence-based adsorbent. A similar trend was observed for the enset root activated carbon (Figure 6d). The removal efficiencies were 96.2% at 20 mg/L, 89.6% at 30 mg/L, 85.4% at 40 mg/L, and 80% at 50 mg/L. This also indicates that increasing the initial Pb(II) concentration resulted in a reduction in the percentage of Pb(II) removed by the root-derived adsorbent.

This observation aligns with findings reported by Ragheb (2007) and others absorbent listed in table 3, regarding Pb(II) ions removal in aqueous solution as adsorbents. Notably, at the lowest initial Pb(II) concentration tested (20 mg/L), the removal efficiency was high for both adsorbents, with the inflorescence-based activated carbon achieving 98.9% removal while the root-based activated carbon achieved up to 96.2% removal efficiency.

Table 3. Comparison of adsorption % Pb(II) ion onto enset inflorescence and root with other different adsorbents found in literatures

Name of adsorbent	%Removal of Pb(II)	Adsorbent dose	References
Alfagrass (stipaTenacissima)	92.39	3.8 g/L	Taziroutand amarani,2009
Need leaves	85	8g/L	Pandhran andNimbalkar,2013
Potato peels	96	4g	Mutungoetal.,2014
Acid treated banana peel	99.53	0.2g/L	Kumarand majumder,2014
Modified orange peel	41.4	4g/L	Mandinaetal.,2013
Raw rice husk	66	70g/L	Nasim et al.,2004
Activated bagasse carbon	99.97	0.8g/L	Nasim et al.,2004
Activated enset inflorescence	95.3	1.5g/L	Present study
Activated enset root	90.3	2g	Present study

Effects of Temperature

Figure 7 indicates that temperature has a noticeable effect on the adsorption of Pb(II) ions onto both types of activated carbon. The inflorescence-based adsorbent shows a trend consistent with an exothermic adsorption process, while the root-based adsorbent displays more intricate temperature dependence, possibly involving a combination of kinetic and thermodynamic factors. The inflorescence adsorbent appears to be more efficient in removing Pb(II) ions across the studied temperatures.

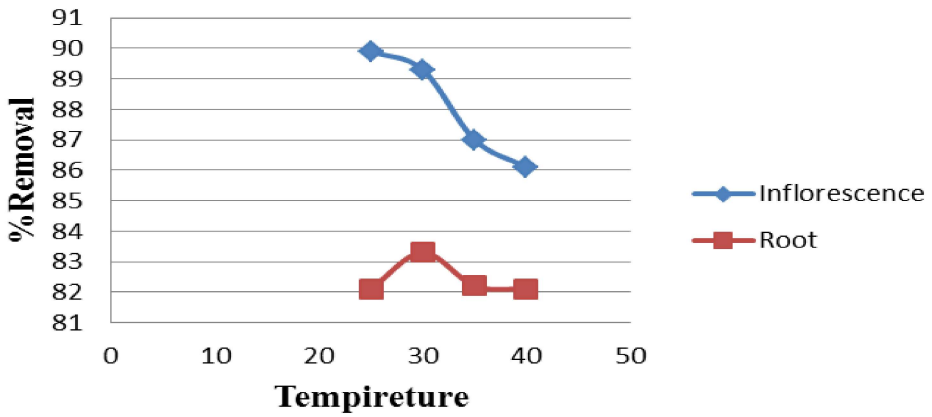

Figure 7. Effect of Temperature removal efficiency of lead at various temperatures

Calculation of Thermodynamic Parameters

To assess energy changes during Pb(II) adsorption, thermodynamic parameters (ΔH, ΔS, and ΔG) were calculated. ΔH and ΔS were obtained from the slope and intercept of the Van't Hoff plot (ln Kd vs. 1/T).

A graph of the natural logarithm of the distribution coefficient (Kd) versus the inverse of temperature (1/T)), using the equation

lnKd = −RTΔH + RΔS. The distribution coefficient (Kd), representing the ratio of adsorbed Pb(II) to the concentration in solution at equilibrium, was calculated. The change in Gibbs free energy (ΔG), which indicates the spontaneity of the adsorption process, was then calculated using ΔG = −RTlnKd. From the Van't Hoff plot Figure 8, although it was previously identified as the Freundlich isotherm plot, this context suggests it's a different figure), the calculated ΔH values were -2.17 kJ mol^{-1} for enset inflorescence and -2.18 kJ mol^{-1} for enset root, while the ΔS values were 32 kJ mol^{-1} and 34.48kJmol^{-1}, respectively, as summarized in Table 4 (a) and (b), which present the adsorption of Pb(II) ions on both activated carbons at different temperatures.

Table 4. Thermodynamic Parameters for enset inflorescence and root at Various Temperatures

(a)						
T(K)	1/T(K^{-1}x10^{-3}	k_d(mLg^{-1})	Lnk_d	ΔH (kJmol)	ΔS (JK1mol)	ΔGkJmol^{-1})
298	3.36	119.7	4.78			-12.2
303	3.3	119.066	4.779			11.8
308	3.25	116	4.75	-2.17	32.409	-11.9
313	3.19	114.8	4.74			--12.3
(b)						
T(K)	1/T(K^{-1}x10^{-3}	k_d(mLg^{-1})	Lnk_d	ΔH ($kJmol^{-1}$)	ΔS ($JKmol^{-1}$)	ΔG ($kJmol^{-1}$)
298	3.36	109.46	4.69			-12.18
303	3.3	111.06	4.71			-12.04
308	3.25	109.6	4.69	-2.18	34.48	-11.6
313	3.19	1106.26	4.666			11.5

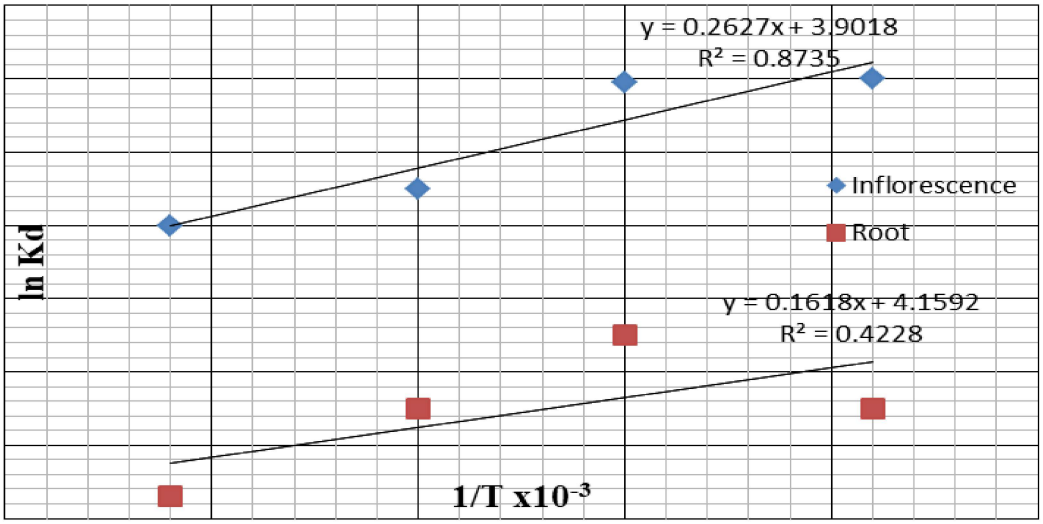

Figure 8. Plot of L kd vs 1/T (pH = 5 and 7 initial concentration = 20mg/L)

The calculated negative enthalpy change (ΔH) indicates that the adsorption of lead ions onto both adsorbents is an exothermic process, meaning it releases heat. The negative values of the ΔG across the tested temperatures, as shown in Table 4, confirm that the adsorption process is spontaneous. Furthermore, the trend of ΔG becoming less negative with rising temperature suggests that the adsorption of lead ions onto these activated carbons is more thermodynamically favorable at lower temperatures. The positive ΔS suggests an increase in randomness at the solid-solution interface as lead ions are adsorbed onto the active sites

Adsorption Isotherm Studies

The equilibrium adsorption of Pb(II) was studied at optimum conditions (pH = 5 and 7 and contact time of 60 min at different concentrations ranging from 20 to 50 mg/L and adsorbent doses of 0.5, 1, 1.5, and 2 g for the metal ions and adsorbent, respectively. The adsorption isotherm can be used to optimize the use of an adsorbent by describing how the solute interacts with the adsorbent (Moreno-Piraján and Giraldo, 2012).

Langmuir Isotherm

The first theoretical model that assumes adsorption will occur at specific homogenous active sites of the sorbent is Langmuir isotherm (Moghadam *et al.,* 2013).

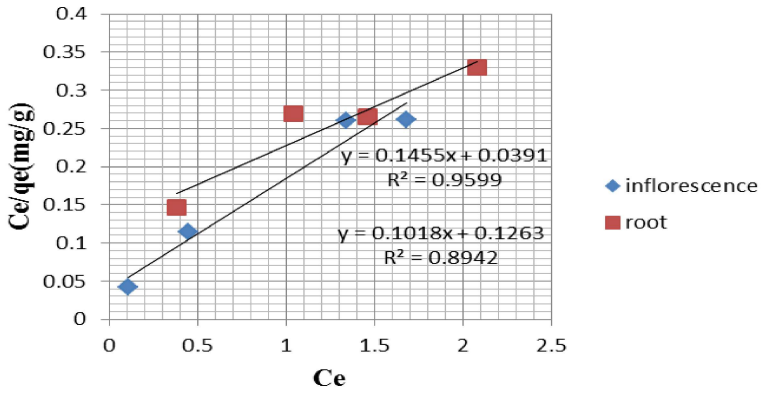

Figure 9. Langmuir isotherm plot for adsorption of Pb(II) ion by Enset inflorescence and Root

The graph plotted between Ce/qe and Ce produces a straight line, where the slope equals 1/qmax and the intercept equals 1/(b × qmax). From this plot, the values of qmax and b can be determined (Figure 9). R^2 values for Pb(II) (0.959 and 0.89 respectively) of enset inflorescence that are greater than 0.90 compared to enset root indicate that the adsorption of these ions onto enset inflorescence follows the Langmuir mode more than enset root.

Freundlich Isotherm

This model describes adsorption occurring on heterogeneous surfaces with varying energy levels, where interactions between adsorbed molecules take place. It assumes that the adsorption sites have an exponential distribution of adsorption energies. The model is described by the following equation (Freundlich, 1907):

$$\text{Log } q_e = \log K_f + 1/n \log C_e$$

Where: q_e is the amount of metal adsorbed by inflorescence and root (mg/g), Ce is the equilibrium adsorbate concentration in mg/L, K_f is the adsorbent capacity measure, and n is the adsorption intensity that can be determined from the linear plot.

The values of the correlation coefficients show that the Freundlich isotherm is appropriate to characterize the adsorption of all the studied metal ions onto inflorescence and root Pb(II) ions, with R^2 = 0.976 and 0.9738 (Figure 10), respectively. The R^2 values of the Freundlich isotherm are somewhat higher than those obtained by the Langmuir isotherm, indicating that this model has better applicability than the Langmuir isotherm model.

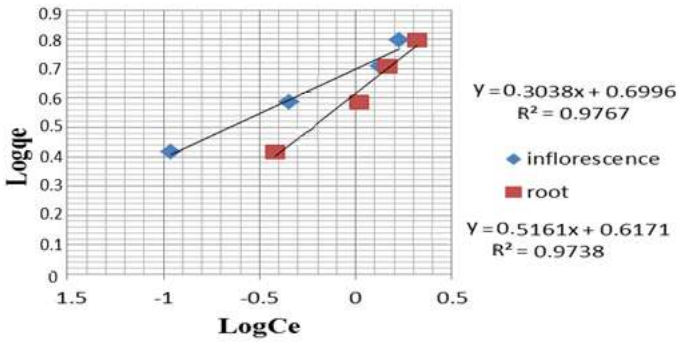

Figure 10. Freundlich isotherm plot for adsorption of Pb(II) ions by enset Inflorescence and root

Table 5. Parameters of Langmuir and Freundlich isotherm on adsorption of metal ions using enset Inflorescence and root adsorbents

Metal	Langmuir		Freundlich	
Pb(II)	b =3.7,1.2 qmax = 25.57,7.9	R^2 =0.959,0.89 RL=0.71,0.68	1/n= 0.308 , 0.516 n = 2.7 , 1.93	K_f = 1.36 ,1.675 R^2=0.973 ,0.978

The Freundlich isotherm's 'n' value provide insights into the favorability of adsorption: values between 2 and 10 indicate good adsorption, 1 to 2 suggests moderately difficult adsorption, and less than 1 implies poor adsorption (Renge *et al*., 2012). For the enset inflorescence, the calculated 'n' value of 2.7 for Pb(II) adsorption (Table 5) falls within the good adsorption range. However, for the enset root see (Table 5), the 'n' value of 1.9 suggests moderately difficult adsorption. Comparing the correlation coefficients (R^2) of the linearized forms of adsorption isotherms ,the Freundlich model demonstrated a better fit (R^2) for Pb(II)

= 0.973 for inflorescence and 0.978 for root) to the experimental equilibrium data for Pb(II) adsorption by both materials, making it the most suitable model to describe this equilibrium. The high R^2 values indicate a good agreement between the experimental data and the Freundlich model. The applicability of the Freundlich model suggests a multilayer adsorption process on the heterogeneous surfaces of both the inflorescence and root activated carbons, implying a non-uniform distribution of adsorption sites with varying energies.

To investigate the controlling mechanism for Pb(II) ion adsorption by enset inflorescence and root activated carbon, the experimental data from this study were analyzed. The pseudo-first-order model, widely recognized for predicting metal adsorption kinetics in both solid and liquid systems, was also applied. (as equation 4.3):

$$\text{Log } (q_e - q_t) = \log q_e - K_1/2.303\ (t) \qquad 4.3$$

The adsorption rate constant can be determined by plotting $\log(q_e - q_t)$ against time (Figure 11).

Adsorption Kinetics

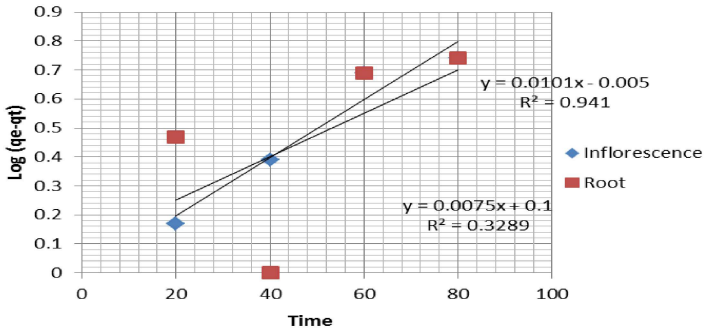

Figure 11. Enset inflorescence and root pseudo 1st order kinetic plot for adsorption of Pb(II) ions

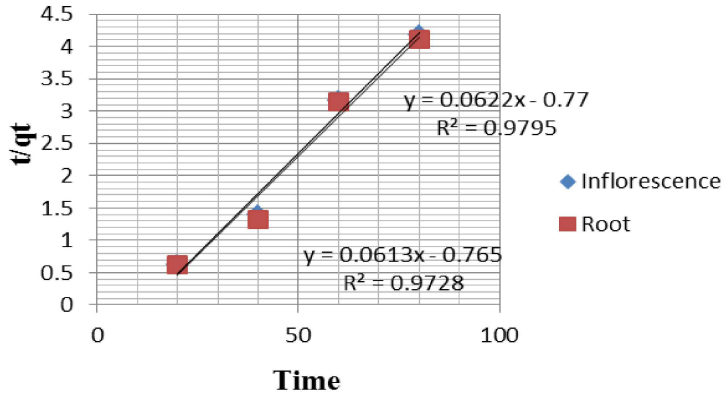

Figure 12. Enset inflorescence and Enset root pseudo 2nd order kinetic plot for adsorption of Pb(II) ion

As shown in Figure 12, R^2 for Pb(II) adsorption using the pseudo-first-order and pseudo-second-order models are 0.941 and 0.328, and 0.979 and 0.972, respectively. Based on these values, the pseudo-second-order model was identified as the best fit for the adsorption process. Using this model, the adsorption capacities and rate constants (k_2) were determined to be 0.003, 0.002, 14.2, and 12.14, respectively.

Conclusion and Recommendation

Activated carbons obtained from freely available enset inflorescence and root, exhibiting alcohol and carboxylic acid functional groups demonstrated significant potential for removing Pb(II) from contaminated water. Under optimized conditions, these materials achieved high removal efficiencies up to 95.3% and 90.3%, for enset inflorescence and root respectively, with a thermodynamically favorable, spontaneous, and exothermic process characterized by increased entropy. The adsorption behavior aligned with the Freundlich isotherm and pseudo-second-order kinetics, suggesting their viability as low-cost adsorbents for broader heavy metal remediation applications.

Conflict of Interests

The author affirms that there are no competing interests or conflicts of interest associated with this publication.

Acknowledgements

The author is grateful to Ambo University for funding this work.

References

Abebe, S., and Dallatu. 2013. Preparation and characterization of palm kernel shell by activation. *Research Journal of Chemistry Science, 3, 54-61.*

Alloway, B. J. (2013). *Heavy metals in soils: Trace metals and metalloids in soils and their bioavailability.* Springer Science & Business Media.

Ahmedna, M. W. 2004. The use of nut shell carbon in drinking water filters for removal of trace metals. *Water Research, 1062-1068.*

Ali, S. A. 2014. The removal of zinc, chromium, and nickel from industrial wastewater using corn cobs. *Journal of Environmental Science, 55(1), 123-131.*

Alluri, H. R. 2007. Biosorption: An eco-friendly alternative for heavy metal removal. *African Journal of Biotechnology, 6, 365-369.*

Avon, J. K. M. (1997). BET surface areas and pore volume distribution of activated carbon. *Journal of Chemical Technology and Biotechnology, 33(3), 335-369.*

B. Sivakumar, C. 2012. Preparation and characterization of activated carbon from Balsamodendron caudatum wood waste through various activation processes. *Rasayan Journal of Chemical Engineering, 3, 321-327.*

Bender, D. 2006. *Dictionary of Nutrition and Technology*. Cambridge, England: Woodhead Publishing.

Bezuneh, T. F. 1966. The production and utilization of the genus enset. Economic Botany, 65-70.

Bog, Danka. 2007. Adsorption of heavy metals from electroplating wastewater by wood sawdust. *Bioresource Technology, 98(2), 402-409.*

Brandt, S. 1993. Enset: Sustainable agriculture in Ethiopia. Proceedings from the International Workshop on Enset held in Addis Ababa (pp. 13-20). Ethiopia.

Browski, A., El Sikaily, A., Khaled, O., and Abdel Wahab. 2001. *Chemical Ecology, 23, 119-129.*

Cox, M. E.-S. E. 2000. Removal of mercury (II) from aqueous solution on a carbonaceous sorbent prepared from flax shive. *Journal of Chemical Technology and Biotechnology, 75, 427-435.*

Dagmawi, M. 2013. Chromium removal from Modjo tannery wastewater using Moringa stenopetala seed powder as an adsorbent. *Water, Air, and Soil Pollution, 224(1719), 1-10.*

Demertzis, K. V. 2011. Nickel removal from wastewater by electrocoagulation with aluminum electrodes. *Journal of Engineering Science and Technology Review, 4(2), 199-192.*

Ferrari, A. O., and Horsfall, M. J. 2011. Preparation and characterization of activated carbon derived from fluted pumpkin stem waste (Telfairia occidentalis Hook f*). Research Journal of Chemistry Science, 1, 1-8.*

Franca, A. O. 2013. Production of adsorbents based on food waste (corn cobs) for

removal of phenylalanine and tyrosine from aqueous solution.

Gashe, B. 1987. Kocho fermentation. *Journal of Applied Bacteriology, 62(6), 43-477*.

Geetha, K. B. 2013. Removal of heavy metals and dyes using low-cost adsorbents from aqueous medium: A review. *Journal of Environmental Research, 4(3).*

Gisi, S. N. 2016. Characterization and adsorption capacities of low-cost sorbents for wastewater treatment. *Sustainable Materials and Technologies, 9, 911-917*.

Gurses, A., and D. C. (2006). Production of granular activated carbon from waste Rosa canina sp. seeds and its adsorption characteristics for dyes. *Journal of Hazardous Materials, 131(1-30), 254-259.*

Hariprasad, P. R. 2016. Preparation of activated carbon from rice husk. *International Research Journal of Engineering and Technology, 3(4).*

Hunduma, T. 2011. Effect of altitude on microbial succession during traditional enset (Ensete ventricosum) fermentation. *International Journal of Food, Nutrition and Public Health, 4(1), 39-53.*

Iqbal, M. A. 2007. Production of an immobilized hydride biosorbent for the adsorption of Ni(II) from aqueous solution. *Process Biochemistry, 42, 148-157.*

Jaishankar, M., Taneja, N., and Sharma, T. 2014. The role of heavy metals in human diseases. *Journal of Toxicology and Environmental Health, Part A, 77(3), 208-232*.

Kadirvelu, K., and K. M.(2003. Utilization of various agricultural wastes for activated carbon preparation and application for the removal of dye and metal ions from aqueous solutions. *Bioresource Technology, 87, 129-132*.

Kanamadi, R. 2010. Removal of hexavalent chromium using coffee husk. *International Journal of Environmental Pollution, 43(1-3), 106-116.*

Kanshie, K. 2002. *Five thousand years of sustainability?* A case study of Gedion land use (southern Ethiopia). Ethiopia: Treemail Publishers.

Karin, Z. 2002. Enset (Ensete ventricosum (Welw.) Cheesman) in subsistence farming systems in Ethiopia. *Conference on International Agricultural Research for Development (pp. 1-6). Ethiopia.*

Keder, M. (2023). *Statistical process optimization on adsorption of phenol from water using activated carbon prepared from false banana (Ensete ventricosum) leaf*. (Master's thesis). Addis Ababa Institute of Technology, Addis Ababa University.

Kidane, S. A., Haukeland, S., Meressa, B. H., Hvoslef-Eide, A. K., & Coyne, D. L. (2021). Planting material of enset (Ensete ventricosum), a key food security crop in southwest Ethiopia, is crucial for the dissemination of plant-parasitic nematode infection. *Frontiers in Plant Science, 12, 664155. doi: 10.3389/fpls.2021.664155*

Kurniawan, T. A. 2006. Physico-chemical treatment techniques for wastewater laden with heavy metals. *Chemical Engineering Journal, 118(1), 83-98.*

Manson, S. 2012. Removal of nickel and cobalt from synthetic drinking water using electrocoagulation technique with alternating current. *International Journal of Chemical Technologies, 4(2), 31-44.*

Mohanty, K., and J. M. 2005. Removal of chromium (II) from dilute aqueous solution by activated carbon developed from Terminal arjuna nuts activated with zinc chloride. *Chemical Engineering Science, 60, 3049-3059.*

Mohammed, A., and Chala, A. 2014. Enset (Ensete ventricosum) production in Ethiopia: Its nutritional and socio-economic importance. *Journal of Food Science and Technology, 51(3), 679-691.*

Muhammad, M. A. 2004. Removal of copper from industrial influent by adsorption with economic viability. Journal of Environmental *Agriculture and Food Chemistry, 3(2), 658-664.*

Mulu, B. D. 2013. Batch sorption experiment: Langmuir and isotherm studies for the adsorption of textile metal ions onto teff (Eragrostis teff) agricultural waste. *Journal of Thermodynamics, 2013, 1-6.*

NB, J. 200. Production and characterization of activated carbon using local agricultural

waste through chemical activation processes. *Industrial and Products, 23, 23-28.*

Nordberg, G. F., Fowler, B. A., Nordberg, M., and Friberg, L. 2007. *Handbook on the Toxicology of Metals (3rd ed.)*. Academic Press.

Olango, T. A. 2014. Indigenous knowledge, use, and on-farm management of enset (Ensete ventricosum (Welw.) Cheesman) diversity in southern Ethiopia. *Journal of Ethnobiology and Ethnomedicine, 10(41), 1-18.*

Ramesh, C. (2011). Adsorption of Zn(II) on activated red mud neutralized by CO2. *Journal of Material Engineering, 266, 93-97.*

Rao, S. 2013. An almost fourth-order parameter-robust numerical method for a linear M2 coupled singularly perturbed reaction-diffusion problem. *International Journal of Numerical Analysis and Modeling, 10(3), 603-621.*

Sahira, J. P. 2011. Preparation and characterization of activated carbon from lapsin seed stone by potassium hydroxide. *Journal of Institute of Engineering, 9(1), 79-88*.

Upadhyay, K. 2006. Solutions for wastewater problems related to the electroplating industry: An overview. *Journal of Industrial Pollution Control, 22(1), 59-66*.

Vanderviere, P. 1998. Chemical coagulation, flocculation, ozonation, oxidation, ion exchange, irradiation, precipitation, and adsorption of heavy metals. *International Journal of the Physical Sciences, 6(31), 59-66.*

Warhurst, A. M., and M. G. 1997. Characterization and application of activated carbon from Moringa oleifera seed husk by single pyrolysis. *Water Research, 31, 759-766.*

Zhang, T., and W. W. (n.d.). Preparation of carbon from forest and agricultural residues through CO2 activation. *Chemical Engineering Journal, 105, 53-59.*